ADVANCED FUNCTIONAL MATERIALS

Organic Solid Solutions: Formation and Applications in Organic Light-Emitting Diodes**

By *Yan Shao* and *Yang Yang**

To enhance the performance of organic devices, doping and graded mixed-layer structures, formed by co-evaporation methods, have been extensively adopted in the formation of organic thin films. Among the criteria for selecting materials systems, much attention has been paid to the materials' energy-band structure and carrier-transport behavior. As a result, some other important characteristics may have been overlooked, such as material compatibility or solubility. In this paper, we propose a new doping method utilizing fused organic solid solutions (FOSSs) which are prepared via high-pressure and high-temperature processing. By preparing fused solid solutions of organic compounds, the stable materials systems can be selected for device fabrication. Furthermore, by using these FOSSs, doping concentration and uniformity can be precisely controlled using only one thermal source. As an example of application in organic thin films, high-performance organic light-emitting diodes with both single-color and white-light emission have been prepared using this new method. Compared to the traditional co-evaporation method, a FOSS provides us with a more convenient way to optimize the doping system and fabricate relatively complicated organic devices.

1. Introduction

Organic compounds have been extensively investigated in the fabrication of various electronic and photonic devices in the last two decades.[1–4] There are currently two widely used methods to enhance device performance: one is the adoption of a multilayer device structure, and the other is the introduction of small amounts of dopants. Organic light-emitting diodes (OLEDs) provide very good examples of these two processes, and device performance has been improved dramatically by doping technology and using proper multilayer structures.[5–7] In the last decade, OLED structures have utilized a graded mixed layer as the active layer to replace the heterojunction, and higher-performance OLEDs with relatively high efficiencies and longer lifetimes have been demonstrated.[8,9] However, device fabrication is becoming more complicated, owing to the necessity to control the dopant(s) and host(s) simultaneously.[8] Herein, we propose a new materials system, a fused organic solid solution (FOSS), which homogeneously blends dopant and host organics through a high-temperature fusion process to form a multicomponent system, and high-performance OLEDs are demonstrated using a stable doping system. This materials system might also be utilized to analyze and understand compound aging behavior under heating, or the device lifetime.

Currently, the most common technology for preparing doped organic thin films is co-evaporation under an ultrahigh vacuum or spin-coating from solution. Dopant concentration plays an important role in device performance; however, the precise control of the dopant concentration over a large area is still a challenging task in manufacturing. This process is further complicated if more than one dopant is involved in the mixed layer.[10,11] Another important issue for doped organic thin films is the proper selection of the host–dopant system.[12,13] In OLEDs, the criteria for materials selection are often determined by the carrier transport and recombination properties, and much attention has been paid to the molecular orbital energy levels, especially the lowest unoccupied molecular orbital (LUMO) and highest occupied molecular orbital (HOMO). On the other hand, some other properties might be neglected, such as material compatibility, which is similar to solubility between two or more chemicals. For example, two small molecules, from which the doped thin films are prepared by co-evaporation, cannot dissolve each other in the solid state, or two polymers which are dissolved in the same solvent cannot form films with uniform morphology after the solvent has volatilized.[14] A seriously incompatible materials system can result in device failure by apparent phase separation in the ultrathin films, especially after a relatively long device operation time. From a practical applications point of view, the proper selection of organic materials will benefit the lifetime of organic devices, which often suffer from stability problems.[15]

2. Results

2.1. Formation and Characterization of Fused Organic Solid Solutions

The formation of a FOSS begins with materials selection. Proper organic materials are selected, and loaded into a high-pressure chamber (as shown in Fig. 1). Upon heating, the mate-

[*] Prof. Y. Yang, Y. Shao
Department of Materials Science and Engineering
University of California
Los Angeles, CA 90095 (USA)
E-mail: yangy@ucla.edu

[**] This research was sponsored by a grant from the US Air Force Office of Scientific Research (AFOSR); grant number F49620-03-0101.

 DOI: 10.1002/adfm.200500032

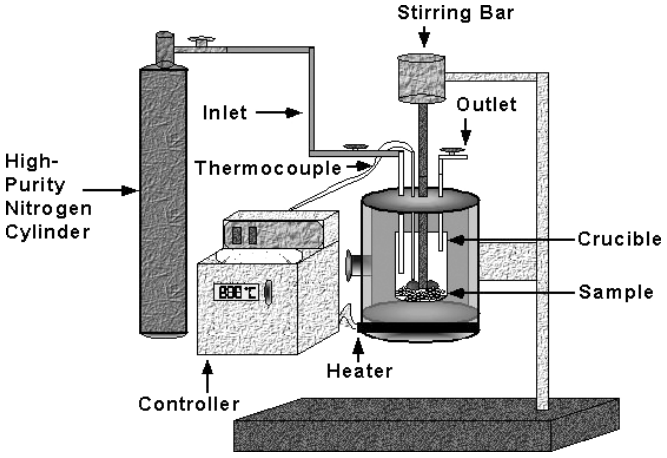

Figure 1. Schematic diagram of the experimental setup for preparing organic solid solutions. A pressurized chamber is the key component in the process of forming the FOSS materials system.

rials form a homogeneous liquid solution under high pressure and high temperature with inert-gas protection. After the melting and mixing process, a FOSS is created by slowly cooling the solution to room temperature. This process provides the system enough time and energy to find its most stable status. Then the created FOSS is checked under a microscope to ensure that there is no phase separation. Not all materials pass this characterization step. Also, not all doping systems can be processed this way, because some organic systems cannot form a liquid phase, even under high pressure. In this case, the FOSS may be obtained by other methods and then the annealing process can be carried out.

In this study, our materials system was comprised of α-naphthylphenylbiphenyl diamine (α-NPD) as the host and 5,6,11,12-tetraphenylnaphthacene (rubrene) as the dopant. This materials system can form a liquid phase under high pressure and temperature, and can then be solidified into a uniform FOSS at room temperature. In the past, tris(8-hydroxyquinoline)aluminum (Alq_3), α-NPD, and rubrene have been demonstrated to be stable and efficient yellow OLED materials.[16] In bipolar-transport-layer[17] and graded-mixed-layer[8] OLEDs, both the electron-transport material (Alq_3) and the hole-transport material (NPD) have been used as the hosts. Hence, we selected NPD and rubrene as the starting materials for the FOSS in this study.

A new apparatus that handles both high temperatures and pressures has been built to carry out the organic fusion process. Figure 1 shows a diagram of the setup. It is known that almost all organic compounds decompose at certain temperatures and many of them are easily sublimed, especially at low pressures, which is disadvantageous for the preparation of FOSSs. To prevent the sublimation of the organic molecules at elevated temperatures, high-pressure nitrogen was applied in the chamber. In our FOSS experimental setup, a pressurized reactor system was employed, with a limitation of 2000 psi (1 psi = 6.895 kPa) pressure at about 400 °C. A temperature controller with a set of thermocouples and a heater can control the vessel temperature automatically. With the help of two windows at an angle of 90° relative to each other, the melting and fusion processes of the samples can be observed.

Details of the processes are described here. First, a mixture of NPD and rubrene with a weight ratio of about 100:2 was ground into a fine powder. The color of the powder looked uniform to the naked eye, but under an optical microscope was observed to be a mixture of fine particles of both NPD and rubrene. The powder mixture showed blue photoluminescence under UV light, which was solely arising from NPD, indicating there was almost no effective energy transfer between NPD and rubrene. In other words, the distance between the two kinds of molecules was beyond the energy transfer radii for Förster excitation transfer (dipole–dipole excitation transfer), which has a very strong dependence on the distance between donor and acceptor.

The powder mixture was then used to prepare a FOSS under a high-pressure nitrogen environment. To prevent oxidation during the fusion process, air was be removed completely from the chamber before heating. High-purity nitrogen (200 psi) was utilized to fill the chamber and then released to purge the system. This procedure was repeated about ten times. The nitrogen gas has two important effects on this process: one is to provide an inert environment to avoid unwanted oxidation; the other is to prevent compound sublimation. For some materials systems, another possible effect of high-pressure nitrogen might be lowering the FOSS processing temperature if the host–dopant materials system has a strong melting-point dependence on the environmental pressure. In other words, if the volume of the mixture becomes smaller upon melting, the melting point under high pressure would be lowered according to the principles of thermodynamics, which would be good for preventing the decomposition of organic molecules.

In our experiment, the mixture of NPD and rubrene was processed for about 20 min under 270 psi pressure at about 225 °C. In this procedure, an orange liquid was observed when the solution of NPD and rubrene was formed. After annealing for 20 min and then cooling to room temperature, the FOSS of NPD and rubrene was ground into a fine powder. It was considered to be a stable materials system, since no phase separation was found under a microscope. The powder was orange and exhibited yellow florescence (like that of rubrene) under UV light, indicating that the energy transfer between NPD and rubrene is almost complete. The melting temperature (T_m) for this system under high-pressure was significantly lowered, so that the molecules could diffuse into each other easily at a relatively low temperature. In this paper, we use "NPD:rubrene" to represent the doped NPD (FOSS), and "NPD:rubrene+Alq_3" to represent the *mixture* of this FOSS and Alq_3.

In order to investigate the thermal characteristics of the host–dopant materials system, several NPD:rubrene FOSSs with different dopant concentrations were prepared by similar methods, and differential scanning calorimetry (DSC) was used to measure the thermal behavior under nitrogen protection. The DSC curve of a pure NPD sample was also measured for reference. In the DSC measurements, each sample was heated to 300 °C at a rate of about 10 °C min^{-1} and rapidly cooled to

ADVANCED FUNCTIONAL MATERIALS

room temperature at a rate of about 50 °C min^{-1}, in order to obtain an amorphous solid sample. The DSC curves were then recorded on heating at a rate of 5 °C min^{-1}. Figure 2a shows the DSC heating curves for doped NPD with different dopant concentrations after cooling from 300 °C to room temperature. Figure 2b shows a detailed diagram of the DSC heating curves for rubrene concentrations of between 0 and 5 %.

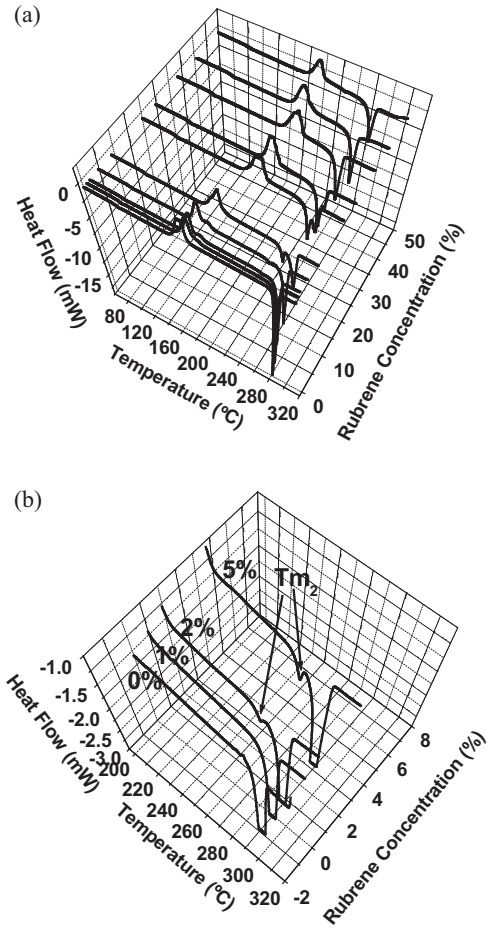

Figure 2. a) DSC heating curves for doped NPD with different dopant concentrations. b) Detailed diagram of the DSC heating curves for rubrene concentrations between 0 and 5 %.

The sharp heat-absorption peak around 281 °C in the NPD curve corresponds to the melting point, and the heat-emission peak located at about 174 °C can be attributed to a phase transformation.[18] The heat-emission peak implies a disorder-to-order process occurring in this phase transformation, since an ordered phase should have a lower free energy. Therefore, between 174 and 281 °C, NPD should be partially crystalline and the phase transformation should be a non-crystal-to-crystal transformation.[18] The two-component system showed an interesting two-melting-point behavior when the rubrene concentration was between 2 and 20 %. In general, the melting point decreased when the dopant concentration in the FOSS increased, although the melting temperature of pure rubrene is higher than that of NPD. All the DSC curves looked similar when the FOSS was in an amorphous state, and the glass-transition temperatures (T_gs) were similar. Figure 3 shows a schematic phase diagram derived from this binary system of NPD and rubrene. There are several phase regions in this diagram. The top phase is the liquid phase (Liq) of FOSS, followed by the partially crystalline (X'tal) and the amorphous phases (Amrph). The region between $T_{X'tal}$ and T_m should be a two-phase (amorphous + crystalline) region, since the non-crystalline organic materials cannot transform into crystalline ones completely. The system showed two phases when the rubrene concentrations were between 2 and 20 %, since there were always two clear melting points for the FOSS.

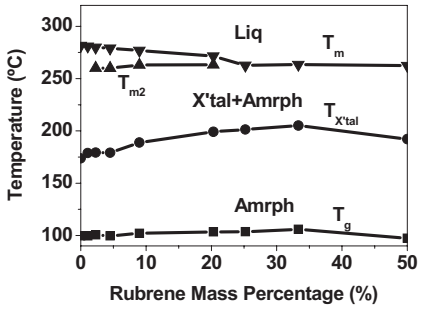

Figure 3. Schematic phase diagram for a binary system of NPD and rubrene generated from the DSC data. T_g is the glass-transition temperature, $T_{x'tal}$ is the crystal-transformation temperature, T_m is the melting point, and T_{m2} is the secondary melting point, or metastable transformation temperature. The top phase is the liquid phase (Liq) of FOSS, which is followed by the crystalline (X'tal) and amorphous phases (Amrph). It is clear that the system shows two phases when the rubrene concentrations are between 2 and 20 %.

2.2. Fabrication of Organic Light-Emitting Diodes Using Fused Organic Solid Solutions

FOSSs are ideal for fabricating OLEDs with a graded junction. Owing to the unique properties of the FOSS material, we were able to fabricate a graded junction using a single evaporation source, which means that only one boat is needed during the process and that the control of evaporation process is rather easy.[19] This single-source evaporation was achieved by evenly premixing the powders of an electron-transport material (Alq_3) and a hole-transport material, in this case *doped* NPD, with rubrene (FOSS), and placing this organic mixture into an evaporation boat. The graded mixed layer is automatically formed when the mixture is evaporated. The formation of a graded mixed layer by this method has been confirmed via UV-vis spectroscopy.[19] The graded junction could be a little sharper than the junction formed by pure NPD and Alq_3 mixture, as doped NPD has a lower melting point than pure NPD, which will have some effect on the vapor pressures. However, UV-vis spectroscopy cannot provide information regarding the graded concentration of rubrene because the concentration is too small. Therefore, we tried to trace the gradient change of the rubrene concentration using photoluminescence, which is strongly concentration dependent.

In order to investigate the graded-junction structures, we designed a special substrate-transport system and shadow mask so that the organic thin films obtained at different evaporation stages could be investigated independently. A series of organic thin films at different stages were prepared via single-source evaporation by moving the quartz substrate sequentially. The deposition rate was about 0.7 Å s^{-1} and the thickness of each film was 30 nm, controlled by a calibrated quartz-crystal monitor. Herein, we define the film prepared from the mixture of Alq_3 and NPD (doped with rubrene) as ANR, and ANR1 is the first 30 nm layer of the graded structure, ANR2 is the second 30 nm layer, and so on. Figure 4a shows the photoluminescence spectra of the thin films prepared from Alq_3 and doped NPD (FOSS). The decreasing intensities between 557 nm and 545 nm indicate the decreasing concentration of rubrene. The blue-shift of the photoluminescence might arise from the effects of interaction between these three materials. The increasing intensities around 520 nm show the increasing concentration of Alq_3. Figure 4b shows a schematic diagram of the distribution of Alq_3 and doped NPD (FOSS) in the graded mixed layer. In order to understand the difference between FOSS and a mixture, a control experiment was carried out. In the control experiment, a *mixture* of NPD and rubrene (2 %) was utilized for a similar deposition and a series of photoluminescence spectra were also obtained. As before, NR1 stands for the first 30 nm layer, NR2 stands for the second 30 nm layer, and so on. Figure 4c shows the photoluminescence spectra of the thin films prepared from such a mixture of NPD and rubrene. It can be seen that only the first 30 nm layer has strong photoluminescence in the yellow range, which means that almost all the rubrene was evaporated after the first 30 nm. This control experiment shows the difference between *FOSS* and a *mixture* of dopant and NPD: there must be some *interaction* between NPD and rubrene molecules in the doped NPD (FOSS), which keeps the doped NPD as a whole during evaporation.

Figure 5 shows the current-density–luminance–voltage (*J–L–V*) curves of an OLED with a NPD:rubrene + Alq_3 graded layer, and the inset plots show the normalized electroluminescence spectrum (upper left) and the efficiency–current-density (μ–*J*, lower right) curve of the device. The device structure was indium tin oxide (ITO)/poly(3,4-ethylenedioxythiophene) (PEDOT): poly(styrene sulfonic acid) (PSS)/NPD:rubrene(2 %)+Alq_3 (80 nm)/Alq_3 (11 nm)/LiF (0.5 nm)/Al (100 nm). The highest efficiency for this kind of device was about 15 cd A^{-1}, and the electoluminescence spectrum was characteristic of rubrene.

To demonstrate white OLEDs prepared using FOSSs,[21] we used α-NPD as the host material, since its energy bandgap is large enough compared to the blue dopants. In our materials system, 4,4′-bis(2,2-diphenylethen-1-yl)biphenyl (DPVBi) was used as the blue-, 10-(2-benzothiazolyl)-2,3,6,7-tetrahydro-1,1,7,7,-tetramethyl-1*H*,5*H*,11*H*[1] benzopyrano[6,7,8-ij]quinolizin-11-one (C545T) as the green-, rubrene as the yellow-, and 4-(dicyanomethylene)-2-*tert*-butyl-6-(1,1,7,7-teramethyljulolidyl-9-enyl)-4*H*-pyran (DCJTB) as the red-emitting dopant. The device structure was ITO/PEDOT-PSS/NPD (30 nm)/doped NPD (40 nm)/bathocuproine (BCP; 4 nm)/Alq_3 (20 nm)/LiF (0.5 nm)/Al (100 nm). The weight ratio was empirically obtained by tracking the chromaticity coordinates and emission spectra from differently doped NPD devices. The optimum weight ratio we obtained for NPD/DPVBi/rubrene/DCJTB/C545T was 100:5.81:0.342:0.304:0.394. Figure 6 shows the electroluminescence spectra from the same white OLED under different current densities ranging from 0.083 to 2.5 mA mm^{-2}. The inset shows the change of CIE (Commission Internationale de l'Eclairage) chromaticity diagram for the white OLED with different current densities (0.083–2.5 mA mm^{-2}).

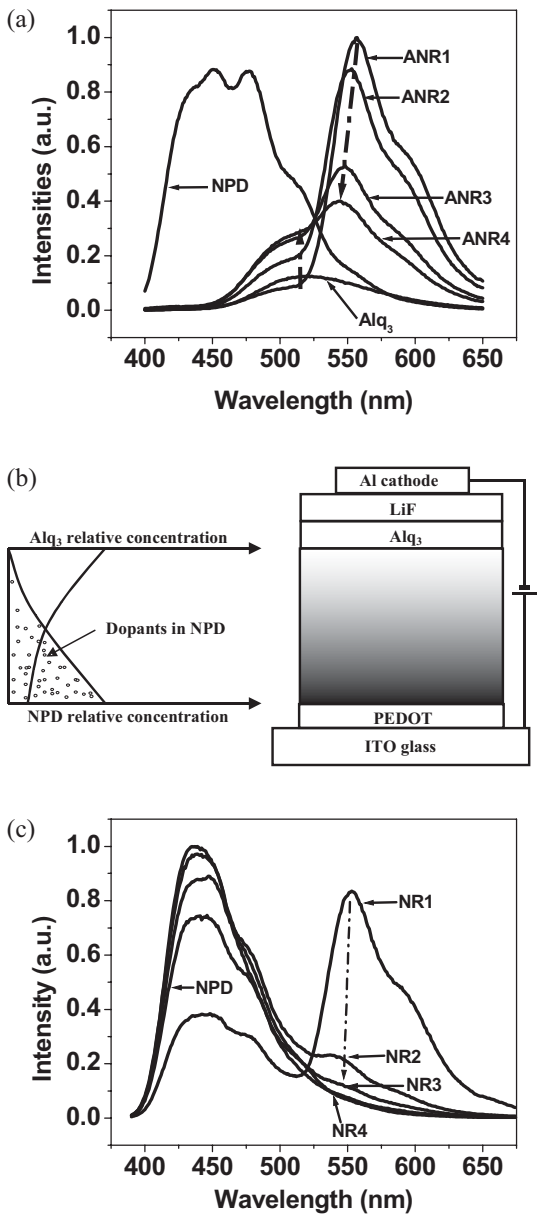

Figure 4. a) Photoluminescence spectra of 30 nm layers obtained at different evaporation stages from a single source including Alq_3 and doped NPD. Also shown are the photoluminescence spectra of pure Alq_3 and NPD 30 nm reference films. b) Schematic diagram for the distribution of Alq_3 and doped NPD in the graded mixed layer, and the structure of the OLEDs. c) Photoluminescence spectra of 30 nm layers for different evaporation stages from a mixture of NPD and rubrene, and pure NPD 30 nm reference films. PEDOT, poly(3,4-ethylenedioxythiophene); ITO, indium tin oxide.

ADVANCED FUNCTIONAL MATERIALS

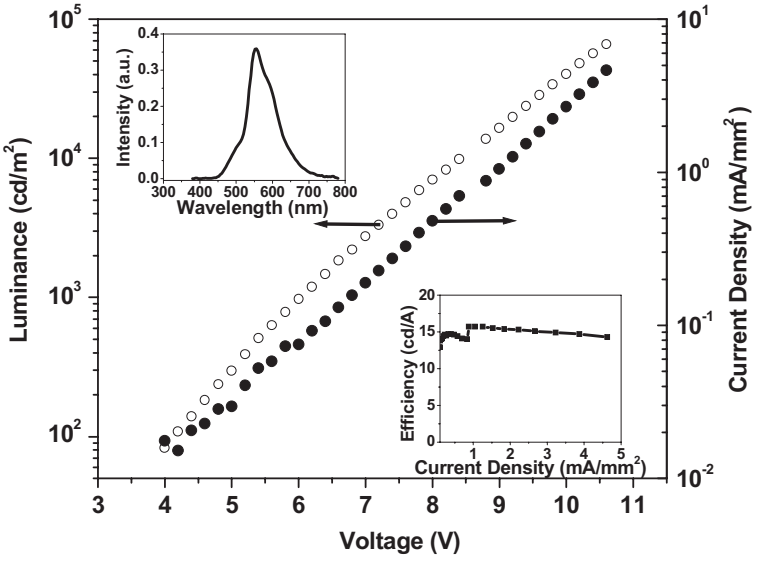

Figure 5. *J–V* and *L–V* curves of the graded-mixed-layer OLED with Alq_3 and rubrene-doped NPD. The inset plots are the EL spectrum (upper left) and μ–*I* curve (lower right).

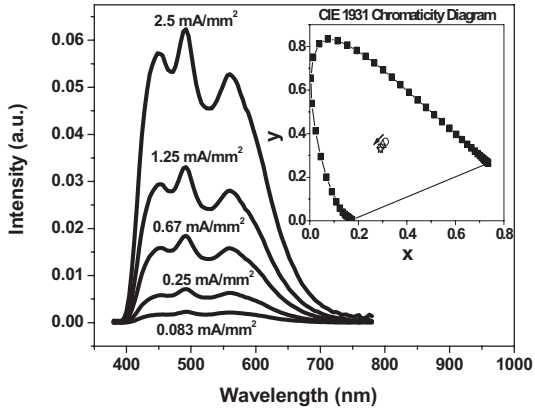

Figure 6. The electroluminescence spectra from the white OLED at different current densities (0.083–2.5 mA mm^{-2}). The inset shows the change of the CIE chromaticity diagram at different current densities (0.083–2.5 mA mm^{-2}) for the white OLED.

3. Discussion

From the DSC diagram of the rubrene and NPD system, we conclude that there is probably no chemical reaction between rubrene and NPD molecules, since this two-melting-point behavior can be repeated exactly upon melting and solidification. It is reasonable to assume there is some reversible interaction between the rubrene and NPD molecules such as π–π stacking. When the mass concentration of rubrene reaches 2 % in the FOSS, this interaction gives a new phase in the FOSS, which has a slightly lower melting temperature than NPD. When the rubrene concentration exceeds 20 %, almost all the FOSS is composed of this new phase, and the FOSS shows only one clear melting point when the concentration reaches 25 %. In other words, when the molecular ratio of NPD and rubrene reaches around 3:1, a new structure is formed. When the total rubrene concentration goes beyond this ratio, every NPD molecule can have strong interactions with rubrene molecules; therefore, there is nothing to distinguish different NPD molecules. The secondary melting points (T_{m2}s) indicate that some metastable phase with a lower melting point is formed in this system at concentrations of rubene of more than 2 %. It is also noteworthy that the crystal-transition temperatures ($T_{x'tal}$s) of NPD:rubrene are clearly higher than that of the pure NPD. This means the FOSS is more difficult to transform from an amorphous state to a crystalline state because the doped molecules serve as defects in the FOSS and hinder the formation of an ordered crystal. The details of each phase are still under investigation. Some other materials systems, including some phosphorescent ones, have shown unstable properties, since serious phase separation can be observed, which would set a barrier for achieving long device lifetimes.

The efficiency of the single-color OLED with rubrene is higher than previously reported graded-mixed-layer OLEDs.[8] This improvement may be attributed to the dopants in NPD, which might serve as hole traps so that a better electron–hole balance can be realized in this structure. The lifetime of this device is enhanced compared to the heterojunction devices, since the sharp interfaces between Alq_3 and NPD have been replaced by a graded structure and the doped NPD films should have better stability in amorphous states than the pure NPD films.

In the white OLED structure, the recombination zone was well-confined, essentially inside the doped NPD layer, especially in the vicinity of the BCP interface; therefore, the emission color was observed to be independent of the thickness of the NPD layer. Owing to the organic-solid-solution processing, the structure was greatly simplified, since the precise control of different evaporation sources at the same time was avoided. White OLED fabrication based on the proposed procedure provides a convenient way for ensuring stable and high-quality color emission. This paper demonstrates only a particular doping system, which includes some common doping materials. Other sophisticated materials systems based on our technique are now being developed and will be reported elsewhere.

4. Conclusions

We demonstrated a novel method to prepare a highly uniform mixed organic solid solution via a high-temperature and high-pressure fusion process. This system could be used to estimate the thermodynamic stability of doping materials. A series of FOSS compounds with NPD doped with rubrene were prepared and DSC was utilized to determine the thermal characteristics. For the first time, the schematic phase diagram for this binary system has been obtained. To demonstrate the useful-

ness of FOSS compounds, high-performance OLEDs were fabricated and the device properties were characterized. FOSS is a novel materials system, for which new organic compounds need to be synthesized to match this process. Therefore, we expect that the device performance will further improve when suitable molecules are available. In addition, compared to the co-evaporation method, this new doping technique can significantly reduce the complexity of fabrication of traditional organic electronic devices.

5. Experimental

DSC measurements were conducted on a DSC 2920 (TA Instruments) and photoluminescence measurements were conducted on a Fluorolog-3 (Instruments S.A., Inc.). Aqueous PEDOT:PSS was Baytron P (commercial name V4071). For the OLED fabrication, ITO-coated glass substrates were treated by a UV–ozone process after sonication in organic solvents. To enhance the injection of holes, a thin PEDOT:PSS [20] film was spin-coated onto the ITO glass with a speed of 4000 rpm (rpm: revolutions per minute) for 1 min and then baked for about 50 min. A bilayer consisting of 5 Å of lithium fluoride and 1000 Å of aluminum was used as the cathode. The device fabrication was carried out under about a 3×10^{-6} torr vacuum, and the deposition rates for organic materials, LiF, and Al were about 3, 0.1, and 7 Å s^{-1}, respectively. The active emitting areas of the OLEDs were about 12 mm^2. The device current-density–voltage (*J–V*) curves were measured using a Keithley 236 source-measurement unit (SMU) controlled by a computer-run program. The brightness and electroluminescence spectra were determined using a Photoresearch 650 photometer.

Received: January 21, 2005
Final version: March 31, 2005
Published online: September 1, 2005

[1] C. W. Tang, S. A. VanSlyke, *Appl. Phys. Lett.* **1987**, *51*, 913.
[2] J. H. Burroughes, D. D. C. Bradley, A. R. Brown, R. N. Marks, K. Mackay, R. H. Friend, P. L. Burns, A. B. Holmes, *Nature* **1990**, *347*, 539.
[3] L. S. Hung, C. H. Chen, *Mater. Sci. Eng.* **2002**, *R39*, 143.
[4] J. N. Bardsley, *IEEE J. Sel. Top. Quantum Electron.* **2004**, *10*, 3.
[5] J. L. Fox, C. H. Chen, *US Patent 4 736 032*, **1988**.
[6] K. Brunner, A. van Dijken, H. Borner, J. J. A. M. Bastiaansen, N. M. M. Kiggen, B. M. W. Langeveld, *J. Am. Chem. Soc.* **2004**, *126*, 6035.
[7] L. S. Liao, K. P. Klubek, C. W. Tang, *Appl. Phys. Lett.* **2004**, *84*, 167.
[8] A. B. Chwang, R. C. Kwong, J. J. Brown, *Appl. Phys. Lett.* **2002**, *80*, 725.
[9] D. Ma, C. S. Lee, S. T. Lee, L. S. Hung, *Appl. Phys. Lett.* **2002**, *80*, 3641.
[10] Y. Hamada, H. Kanno, T. Tsujioka, H. Takahashi, T. Usuki, *Appl. Phys. Lett.* **1999**, *75*, 1682.
[11] T. Ali, G. Jones, W. Howard, *SID 04 Digest* **2004**, 1012.
[12] C. W. Tang, S. A. VanSlyke, C. H. Chen, *J. Appl. Phys.* **1989**, *65*, 3610.
[13] G. He, O. Schneider, D. Qin, X. Zhou, M. Pfeiffer, K. Leo, *J. Appl. Phys.* **2004**, *95*, 5773.
[14] L. D. Bozano, K. R. Carter, V. Y. Lee, R. D. Miller, R. DiPietro, J. C. Scott, *J. Appl. Phys.* **2003**, *94*, 3061.
[15] G. Vamvounis, H. Aziz, N. Hu, Z. D. Popovic, *Synth. Met.* **2004**, *143*, 69.
[16] Z. D. Popovic, H. Aziz, *IEEE J. Sel. Top. Quantum Electron.* **2002**, *8*, 362.
[17] V.-E. Choong, S. Shi, J. Curless, C.-L. Shieh, H.-C. Lee, F. So, J. Shen, J. Yang, *Appl. Phys. Lett.* **1999**, *75*, 172.
[18] D. S. Qin, D. H. Yan, L. X. Wang, *Appl. Phys. Lett.* **2000**, *77*, 3113.
[19] Y. Shao, Y. Yang, *Appl. Phys. Lett.* **2003**, *83*, 2453.
[20] A. Elschner, F. Bruder, H.-W. Heuer, F. Jonas, A. Karbach, S. Kirchmeyer, S. Thurm, R. Wehrmann, *Synth. Met.* **2000**, *111*, 139.
[21] Y. Shao, Y. Yang, *Appl. Phys. Lett.* **2005**, *86*, 073 510.

